JOURNAL OF MATERIALS SCIENCE **35** (2000) 1675–1684

The measurement of the micro-fibril angle in soft-wood

K. M. ENTWISTLE
University of Manchester/UMIST Materials Science Centre, Grosvenor Street, Manchester M1 7HS, UK
E-mail: ken.entwistle@man.ac.uk

N. J. TERRILL
CLRC Daresbury Laboratory, Daresbury, Warrington WA, UK
E-mail: n.j.terrill@dl.ac.uk

The paper explores the measurement, using X-rays, of the micro-fibril angle of the cellulose fibres in the S2 layers of the cell walls of soft-wood, particularly pinus radiata. It is demonstrated that unambiguous values of the micro-fibril angle can be obtained from small angle X-ray scattering patterns if the X-ray beam is directed at 45 degrees to both sets of cell walls, with the cell axes vertical. The theory of the method is presented and justified. Examples of the measurement of the micro-fibril angle in pinus radiata specimens are given. It is demonstrated that the scattering patterns obtained with the X-ray beam directed normal to one set of cell walls are not capable of yielding micro-fibril angle values. The wide-angle diffraction pattern from the (002) planes with the X-ray beam equally inclined to both sets of cell walls has been analysed. The analysis has been justified experimentally and it is shown that the S2 fibres give rise to eight intensity maxima round the (002) circle and that the azimuthal angles can be related to the micro-fibril angle. It has not been possible to resolve the eight peaks. Wide-angle diffraction patterns revealed four peaks, each comprising two merged adjacent peaks. The azimuth angle at the centre of each of the four peaks is the average of those for the two constituent peaks. It is demonstrated that values of the micro-fibril angle can be obtained from this average azimuth angle.

1. Introduction

The individual cells of softwood, of which pinus radiata is an important example, are rectangular in section, 20–60 μm across, and about 3 mm long. A cell wall (see Fig. 1) comprises three layers, designated S1, S2 and S3.Where two walls of adjacent cells join there are six layers, two each of S1, S2 and S3. The layers comprise natural cellulose filaments embedded in a matrix of lignin and hemicellulose. The cellulose fibres in the S1 and S3 layers lie roughly at right angles to the cell axis. The fibres in the S2 layers form helices making an angle M, called the micro-fibril angle, to the axis of the cell. Micro-fibril angles are typically in the range 10 to 40 degrees. The sets of fibres in the two S2 layers of one wall lie in mirror image orientation relative to the cell axis. About 80% of the cellulose lies in the S2 layers. Since cellulose has a higher elastic modulus than lignin or hemicellulose, it would be expected that the cellulose fibrils in the S2 layers dominate the elastic stiffness of wood specimens. Convincing evidence is emerging that this is the case and, in particular, the modulus is sensitively affected by the micro-fibril angle in the S2 layers. If the micro-fibril angle is small, the elastic modulus along the grain is high because it is simply determined by the elastic modulus and the volume fraction of cellulose. If the micro-fibril angle is large, the fibres in S2 behave like close-coiled springs and the modulus is low. Changes of micro-fibril angle can result in modulus changes by a factor of at least five.

Professor Jeremy Astley of the Mechanical Engineering Department of the University of Canterbury in New Zealand is modelling the cell structure of pinus radiata and is applying finite element analysis to the model to predict the nine elastic constants of this orthotropic material. It emerges clearly from this analysis that the micro-fibril angle of the cellulose in the S2 layers plays a dominant part in determining the values of the elastic constants.The Manchester Materials Science Centre is collaborating in this project by making measurements of elastic constants on clearwood samples to compare with the predictions of the model. It is also making measurements, in collaboration with the Synchrotron Laboratory at Daresbury, of the micro-fibril angle of the elasticity specimens. This paper is concerned with the micro-fibril angle measurements.

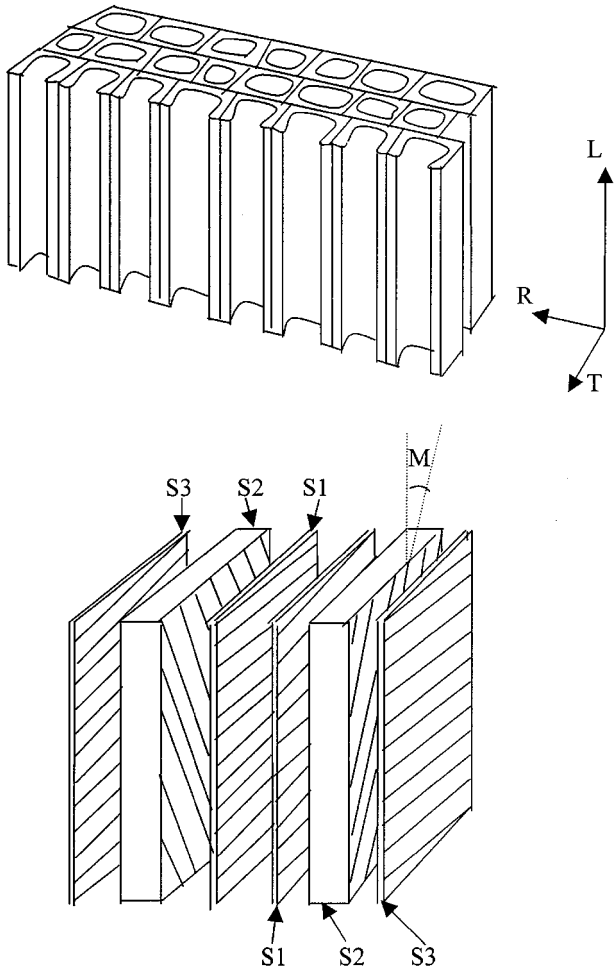

Figure 1 Diagram showing the shape of the soft-wood cells and the composite structure of the cell walls. L, R and T are respectively the longitudinal, the radial and the tangential directions in the cross-section of the tree.

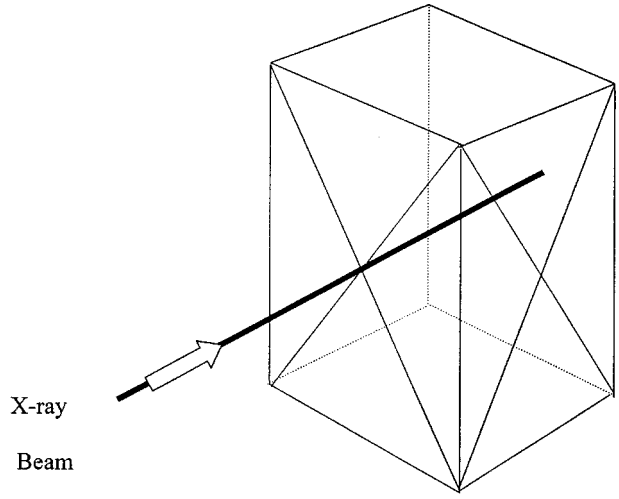

Figure 2 Diagram of a cell with the X-ray beam directed normally to one set of cell walls.

2. Measurement of micro-fibril angle

A number of techniques for the measurement of micro-fibril angle have been reported. Individual cell walls can be exposed by microtoming and the cellulose fibres can be decorated with either iodine [1] or mercury and the fibre orientation can be measured microscopically. Alternatively polarised light [2] can be used. Also infra-red spectroscopy [3] has recently been reported as a possible technique for micro-fibril angle measurement.

By far the most commonly used technique, however, is wide-angle X-ray scattering (WAXS) using the reflection from the (002) planes. This technique was pioneered by Cave [4] who made important contributions to its understanding. The method based on Cave's analysis was explored by Melan [1]. He verified Cave's method by making parallel measurements of micro-fibril angle using the iodine staining method and X-rays. We discuss this method below. This discussion leads us to propose an alternative approach.

3. Wide-angle X-ray scattering

Natural cellulose is monoclinic. The approximate unit cell dimensions are $a = 0.835$ nm , $b = 1.03$ nm and $c = 0.79$ nm. The angle between the c and the a axes is 84 degrees. The b direction lies along the fibre axis. The strongest X-ray reflection from the cellulose crystal is from the (002) planes, which reflect at a Bragg angle of 11.3 degrees with Cu K_α radiation. The normal to the (002) planes is perpendicular to the b direction, that is perpendicular to the fibre axis, so for a vertical fibre the (002) diffraction spots will lie in the equatorial plane. Weaker reflections occur from the (101) and the $(10\bar{1})$ planes whose normals are also perpendicular to the fibre axis. There is also a strong (021) reflection and a weak (040) reflection which lies on the meridian of the diffraction pattern for a vertical fibre. Cave has suggested using the (040) reflection to measure the micro-fibril angle.

Consider now the X-ray scattering from a wood sample with the axis of the cells aligned vertically and the X-rays incident normally on one set of cell walls (see Fig. 2) which we shall call the front walls. The cellulose fibres in the S2 layers of the front walls will produce diffraction spots in an azimuthal direction perpendicular to their length. The spots will be extended along the (002) diffraction ring because the fibrils that make up the fibres will wander slightly around the axial direction. Cave assumes that this will produce a distribution of intensity round the diffraction ring that is Gaussian. The position of peak intensity of the spots from the two sets of fibres in the S2 layers will be separated by an azimuth angle equal to twice the micro-fibril angle. So if the position of the peak intensity in each spot could be located the micro-fibril angle could be measured directly. This turns out not to be possible, in the range of micro-fibril angles of practical importance, because the (002) diffractions from the cellulose fibres in the other set of cell walls that are parallel to the X-ray beam, that we shall call the side walls, obscures the peaks. We show later that the (002) diffraction from the S2 fibres in the side walls lie at azimuth angles between about $+10$ degrees to -10 degrees of the equator of the diffraction pattern. The effect of this is to give a continuous arc of intensity on the (002) diffraction circle which is the sum of the front wall and the side wall diffractions.

Cave has suggested that the extreme edges of the (002) arcs will contain only the side of the Gaussian

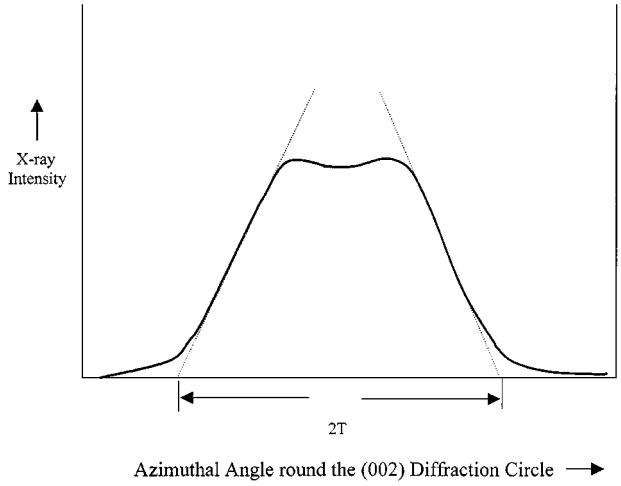

Figure 3 Diagram defining the angle 2T, which is the distance between the points of intersection with the zero intensity axis of the two tangents drawn at the steepest point on the flanks of the intensity distribution.

intensity distribution of the (002) spots from the S2 fibres in the front walls and will not be contaminated by the side wall diffractions. With this in mind, he proposes that the tangents at the steepest points at the edges of the intensity arcs (see Fig. 3) will intersect the zero intensity axis at points separated by the angle $2T$. This can be related to $2M$, the angular separation between the peaks of the front wall S2 spots, which is twice the micro-fibril angle. Cave asserts that $M = 0.6T$. He arrives at this relation from the fact that the tangent to the steepest point on a Gaussian curve intersects the zero axis at a distance from the peak equal to the standard deviation σ. So $2T = 2(M + \sigma)$. By making an assumption about the value of σ Cave arrives at his result. Meylan has tested the Cave relation by carrying out iodine staining and x-ray measurements on the same specimens and confirms that the relation $M = 0.6T$ provides a valid basis for extracting values of micro-fibril angle from WAXS data.

A further complication in the diffraction pattern from wood samples is that the cellulose fibres in the S1 and S3 layers, which lie almost horizontally, will produce (002) diffractions which are close to the meridian line. This will not seriously interfere with the S2 layer diffractions except for very large micro-fibril angles where the spread of the (002) arcs is great.

4. Alternative approaches to the measurement of micro-fibril angle

We have explored the possibility of developing methods of measuring the micro-fibril angle that avoid problems from overlapping intensity peaks. We first look at wide-angle diffraction and then address small angle X-ray scattering.

5. Wide-angle X-ray scattering

We now calculate the geometry of the (002) diffraction pattern produced by a wood specimen when the incident X-rays are directed at 45 degrees to both sets of cell walls. We will show that there are eight discrete (002)

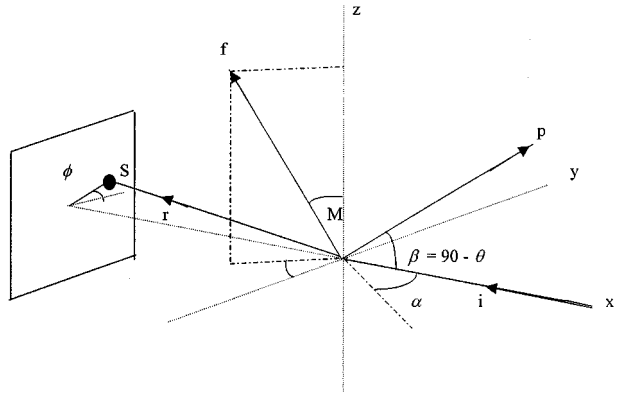

Figure 4 Diffraction from a single cellulose fibre.

spots arising from the four sets of cellulose fibres. If the azimuth angle of these spots can be measured then the micro-fibril angle can be extracted. We begin by analysing the diffraction by a single cellulose fibre in an arbitrary orientation relative to the X-ray beam.

6. Diffraction from a single fibre

The fibre and the X-ray geometry is shown in Fig. 4. We set up the orthogonal co-ordinate axes (x, y, z). The z axis is the direction of the axis of a wood cell. The cell wall, shown as a dotted rectangle, lies along the cell axis and its normal lies at an angle α to the incident X-ray beam i which is directed along the x axis. We consider a single cellulose fibre f lying in the cell wall and at an angle M to the cell axis, which is the z direction; M is the micro-fibril angle that we seek to measure.

The normal to the reflecting (002) planes are perpendicular to f. The particular set of (002) planes that reflect under the geometrical conditions illustrated will be those whose normals lie at $\beta = 90 - \theta$ to the incident X-ray beam i where θ is the Bragg angle.The normal that satisfies that condition is p. The reflected ray r lies at the angle 2θ to the x axis and will produce the diffraction spot S on the detector plane, which is shown as the solid rectangle. The azimuth angle of S relative to the y axis direction is ϕ. Our task is to relate ϕ and M, and to establish how ϕ varies with α as the cell wall is rotated about the z axis.

The critical fact used in the analysis is that the Bragg reflection condition requires that the vectors $\boldsymbol{i}$, $\boldsymbol{p}$ and $\boldsymbol{r}$ must lie in the same plane. The vector product $(\boldsymbol{i} \wedge \boldsymbol{p})$ is a vector perpendicular to both $\boldsymbol{i}$ and $\boldsymbol{p}$. But since $\boldsymbol{r}$ is in the same plane as $\boldsymbol{i}$ and $\boldsymbol{p}$, $\boldsymbol{r}$ must be perpendicular to the vector $(\boldsymbol{i} \wedge \boldsymbol{p})$ also. In that case, the scalar product of orthogonal vectors being zero,

$$(\boldsymbol{i} \wedge \boldsymbol{p}) \cdot \boldsymbol{r} = 0$$

The direction cosines of the vectors are

$$\boldsymbol{i} = (1, 0, 0)$$

$$\boldsymbol{p} = (\cos\beta, m, n)$$

$$\boldsymbol{r} = (-\cos 2\theta, \sin 2\theta \cos\phi, \sin 2\theta \sin\phi)$$

In matrix form ($\boldsymbol{i} \wedge \boldsymbol{p}$) is, where $\boldsymbol{i}$, $\boldsymbol{j}$ and $\boldsymbol{k}$ are unit vectors along the x, y and z axes respectively, the vector

$$\begin{bmatrix} \boldsymbol{i} & \boldsymbol{j} & \boldsymbol{k} \\ 1 & 0 & 0 \\ \cos\beta & m & n \end{bmatrix} = 0 - \boldsymbol{j}n + \boldsymbol{k}m$$

The scalar product of this vector and the vector $\boldsymbol{r}$ is the following, and we have seen that it must be zero so

$$0 - n\ \sin 2\theta\ \cos\phi + m\ \sin 2\theta\ \sin\phi = 0$$

and

$$\frac{n}{m} = \tan\phi \quad \text{or} \quad n = m\ \tan\phi$$

For the vector $\boldsymbol{p}$

$$l^2 + m^2 + n^2 = 1$$

that is

$$\cos^2\beta + m^2 + m^2\ \tan^2\phi = 1$$
$$\cos^2\beta + m^2\ \sec^2\phi = 1$$
$$m^2\ \sec^2\phi = 1 - \cos^2\beta = \sin^2\beta$$

but

$$\sin\beta = \cos\theta$$

so

$$m^2 = \cos^2\phi\ \cos^2\theta \quad \text{and} \quad m = \pm\cos\phi\ \cos\theta$$

We see by inspection of the particular geometry of Fig. 4, that m is positive so we take the value

$$m = +\cos\phi\ \cos\theta$$

Substituting this value for m and also $n = m\ \tan\phi$, the direction cosines of the vector $\boldsymbol{p}$ become

$$(\sin\theta, \cos\phi\ \cos\theta, \cos\phi\ \cos\theta\ \tan\phi)$$

where we have equated $\cos\beta$ to $\sin\theta$.

Now since the pole of the reflecting (002) planes is perpendicular to the fibre axis, the vectors $\boldsymbol{p}$ and $\boldsymbol{f}$ are perpendicular so their scalar product is zero

$$\boldsymbol{p} \cdot \boldsymbol{f} = 0$$

The direction cosines of $\boldsymbol{f}$ are

$$(-\sin M\ \sin\alpha, -\sin M\ \cos\alpha, \cos M)$$

So

$$\boldsymbol{p} \cdot \boldsymbol{f} = -\sin\theta\ \sin M\ \sin\alpha - \sin M\ \cos\alpha\ \cos\phi\ \cos\theta + \cos M\ \sin\phi\ \cos\theta = 0$$

This equation yields

$$\cot M = \frac{1}{\sin\phi}\{\tan\theta\ \sin\alpha + \cos\phi\ \cos\alpha\} \qquad (1a)$$

This is the relation we seek. Note that if $\alpha = 0$, which corresponds to the x-ray beam normally incident on the cell wall,

$$\cot M = \cot\phi \quad \text{and} \quad M = \phi$$

so the azimuth angle in the diffraction pattern is equal to the micro-fibril angle, which is the expected result.

If $\alpha = 90$ degrees. which means that the X-ray beam is parallel to the cell wall,

$$\sin\phi = \frac{\tan\theta}{\cot M}$$

so, for example, if $M = 40$ degrees, which is a large micro-fibril angle, $\phi = 9.6$ degrees. This illustrates the earlier statement that the diffraction from the side-walls lies between the diffraction arcs from the S2 fibres in the front walls.

In addition to the diffraction spot S from the (002) plane with pole $\boldsymbol{p}$ in Fig. 4, there is another set of planes with normals $\boldsymbol{p}^{|}$ (see Fig. 5) which also satisfy the Bragg condition where again $\beta = 90 - \theta$. This corresponds to taking the negative value for the direction cosine m in the vector for the pole of the reflecting planes. That pole is $\boldsymbol{p}^{|}$ in Fig. 5. The planes of the pole give a diffraction spot $\boldsymbol{S}^{|}$ with an azimuth angle, as defined in Fig. 5 of $\phi^{|}$. The direction cosines of the vectors are

$$\boldsymbol{i} = (1, 0, 0)$$
$$\boldsymbol{p}^{|} = (\cos\beta, m, n) = (\sin\theta, m, n)$$
$$\boldsymbol{r} = (-\cos 2\theta, -\sin 2\theta\ \cos\phi^{|}, -\sin 2\theta\ \sin\phi^{|})$$
$$\boldsymbol{f} = (-\sin M\ \sin\alpha, -\sin M\ \cos\alpha, \cos M).$$

And if we perform the analysis following the steps of the previous case, noting by inspection of Fig. 5 that we must take the negative value of the direction cosine m, we find

$$\boldsymbol{p}^{|} = (\sin\theta, -\cos\theta\ \cos\phi^{|}, -\cos\theta\ \sin\phi^{|})$$

and

$$\cot M = \frac{1}{\sin\phi^{|}}(\cos\phi^{|}\ \cos\alpha - \tan\theta\ \sin\alpha) \qquad (1b)$$

This relation differs from Equation 1a and so ϕ is not equal to $\phi^{|}$ for given values of M and α, and therefore

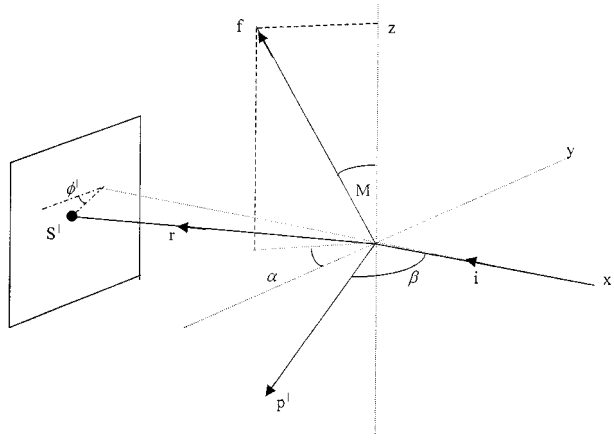

Figure 5 The alternative diffraction to Fig. 4.

for a single fibre the two (002) spots are not diametrically opposite.

If we calculate, for example, the values of ϕ and $\phi^{|}$ for $\alpha = 45$ degrees and $M = 45$ degrees, we find $\phi = 41.9$ degrees and $\phi^{|} = 28.6$ degrees. So the (002) diffraction pattern is

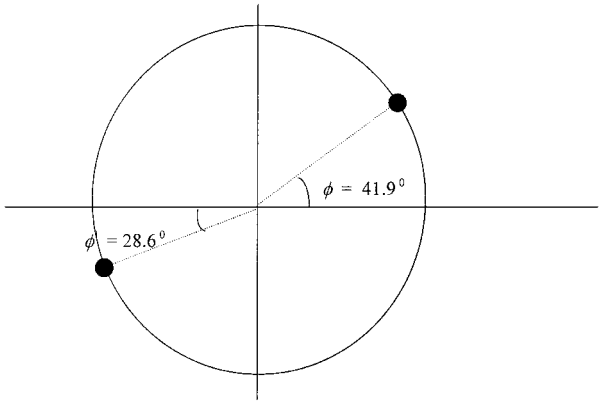

An experiment was carried out to check these predicted azimuth angles. A narrow ribbon of parallel cellulose fibres from the stem of the Common Nettle (*Urtica dioica*) was mounted on a square open frame. This was fixed on the top of a goniometer head which provided rotation about a vertical and a horizontal axis. With this arrangement the set of fibres could be oriented in the X-ray beam to simulate a single set of fibres in a single cell wall with any desired value of M and α. Fig. 6 shows the diffraction pattern produced with $M = 45$ degrees and $\alpha = 45$ degrees and the fibre oriented in a direction relative to the X-ray beam corresponding to "d" in Fig. 9. The two azimuth angles were measured on the film by superimposing on it the diffraction pattern for a vertical fibre, which defined the equatorial direction. The measured values of the azimuth angles were $\phi = 29.0^{\circ}$ and $\phi^{|} = 41.5^{\circ}$, which are in good agreement with the predicted values.

With the theory thus confirmed we can proceed to calculate

(a) How the two azimuth angles ϕ and $\phi^{|}$ vary with the micro-fibril angle M for a parallel set of fibres at 45 degrees to the X-ray beam. This relation is plotted in Fig. 7.

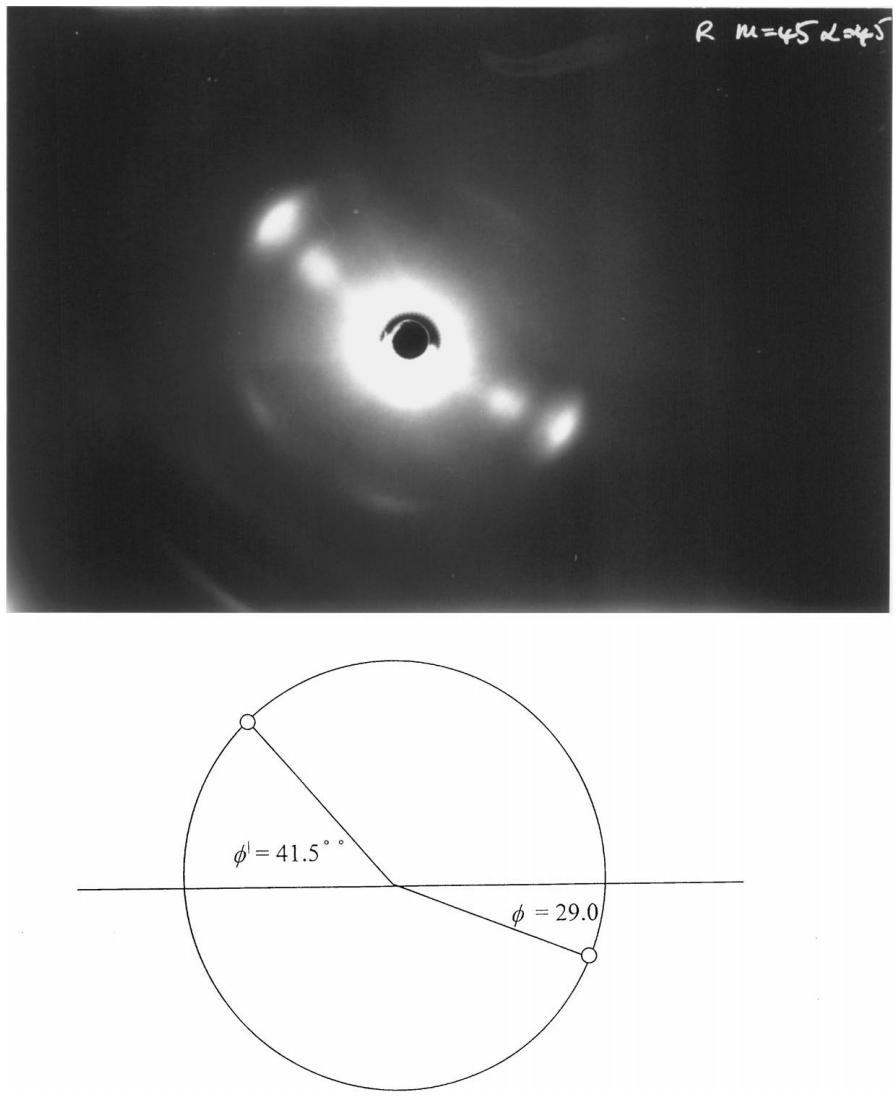

Figure 6 Wide-angle diffraction pattern from a set of parallel cellulose fibres oriented with $M = 45$ degrees and $\alpha = 45$ degrees and corresponding to the set of fibres designated "d" in Fig. 9. The lower diagram shows the measured azimuth angles.

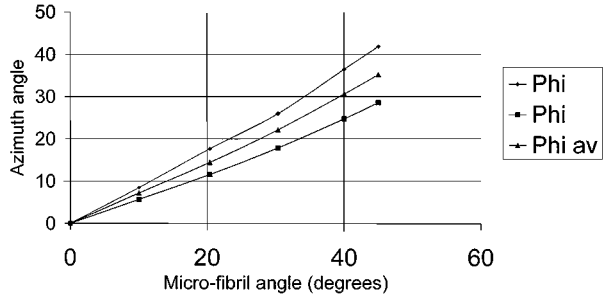

Figure 7 Relation between the micro-fibril angle and the two azimuth angles for a single fibre in a cell wall at 45 degrees to the X-ray beam. Triangular points are the mean.

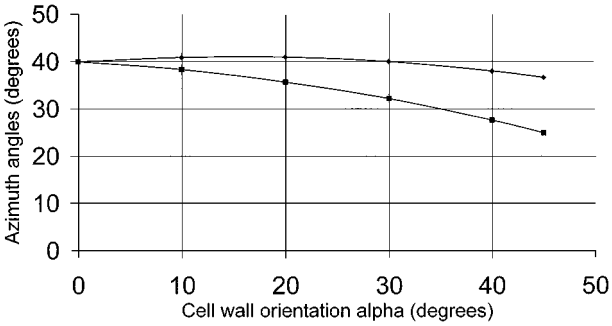

Figure 8 Variation of the two azimuth angles with the cell wall orientation for a micro-fibril angle of 40 degrees.

(b) How the two azimuth angles vary with α, the orientation of the cell wall for a given value of M. The result of such a calculation for $M = 40$ degrees is plotted in Fig. 8.

7. The WAXS patterns from a wood specimen

From equations equivalent to (1a) and (1b) we can work out the form of the diffraction pattern that would be produced from a wood specimen oriented so that the cell axes are vertical and and both sets of cell walls are equally inclined at 45 degrees to the incident X-ray beam. There will be four sets of S2 fibres in the two sets of cell walls. An individual fibre of each set, labelled a to d, is drawn in Fig. 9. Each fibre will give two diffraction spots, so there will be eight spots round the (002) circle. The calculated distribution of the spots for $M = 45$ degrees and $\alpha = 45$ degrees is displayed in the following diagram (Fig. 10).

We have attempted to resolve the eight intensity maxima in the wide-angle diffraction patterns. These measurements yielded an intensity plot round the (002) diffraction circle that had four maxima, each comprising two peaks that were not resolved. The azimuth angle at the centre of each peak will lie mid-way between the azimuth angles of the two constituent peaks and this angle can be related to the micro-fibril angle. That relationship can be derived from Equations 1a and 1b. For $\alpha = 45$ degrees

$$\phi_{\text{av}} = \left(\frac{\phi + \phi^{|}}{2}\right) = \text{A tan}\left(\frac{(\tan M)}{\sqrt{2}}\right). \qquad (2)$$

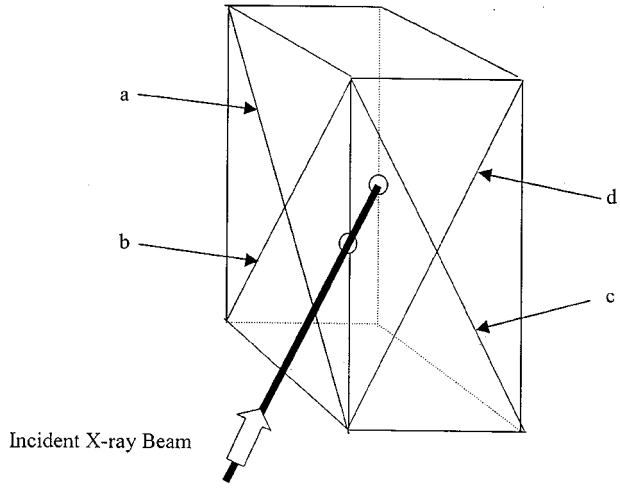

Figure 9 Diagram showing the four sets of cellulose fibres, labelled a to d, in the two sets of cell walls. The X-ray beam is directed at 45 degrees to both sets of walls.

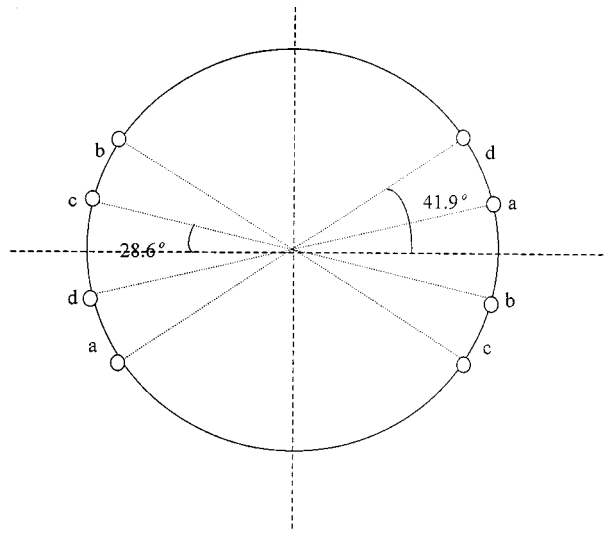

Figure 10 Location of the (002) diffraction spots for the four sets of cellulose fibres when the X-ray beam is equally inclined to both sets of cell walls and the cell axes are vertical.

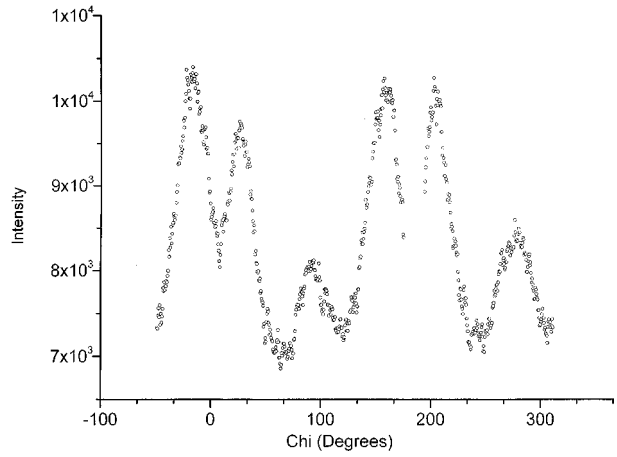

Figure 11 Intensity variation round the (002) diffraction circle for a pinus radiata specimen with the X-ray beam directed at 45 degrees to both sets of cell walls.

All four double peaks will lie at this azimuth angles to the equator of the diffraction pattern. The variation of ϕ_{av} with M is plotted in Fig. 7.

The measured intensity round the (002) diffraction circle in the wide-angle diffraction pattern for a pinus radiata specimen with the cell walls oriented at 45 degrees to the X-ray beam is shown in Fig. 11. The four intensity maxima derived from the S2 fibres are evident along with broader and lower maxima from the S1 and S3 fibres. The angle between the mid-points of the adjacent pairs of S2 maxima is 43.4 degrees, so the average value of ϕ is $\phi_{av} = 21.7$ degrees. This, from Equation 2, corresponds to a micro-fibril angle of 29.4 degrees.

To make an interesting comparison, the same specimen was irradiated with the X-ray beam perpendicular to one set of cell walls. The intensity distribution round the (002) diffraction circle is shown in Fig. 12 and reveals the broad (002) arcs. The micro-fibril angle was obtained by Cave's method. The length of the intercept $2T$ with the zero intensity line made by the lines of steepest gradient at the flanks of the S2 intensity distribution is 99.7 degrees so $T = 49.9$ degrees. Then the micro-fibril angle $M = 0.6T = 29.9$ degrees. This is close to the previous value obtained from the diffraction pattern produced with the X-ray beam at 45 degrees to the cell walls.

The advantage of measurement using the latter irradiation geometry is that it does not require the determination of the background intensity which is required for the Cave method.

In the next stage in the project we explored the potential of small angle X-ray scattering for the measurement of micro-fibril angle.

8. Small angle X-ray scattering

The cellulose fibrils are about 25 nm diameter and about 10^5 longer than that, so the small angle X-ray scattering from a straight fibre produces intensity streak on the recording plane in the plane of the cross-section of the fibre. With a two-dimensional detector plate with its normal parallel to the incident X-ray beam, a single vertical fibre will produce an intensity streak in the horizontal plane. The scattering angle θ at the minimum of the radial intensity distribution for a circular section fibre of cross-section radius R is given by the relation

$$\frac{3.83}{R} = \frac{4\pi}{\lambda} \sin\frac{\theta}{2}$$

For $\lambda = 0.15$ nm, which is the wavelength used in the Daresbury Synchrotron, and $R = 1.25$ nm this gives $\theta = 4.1$ degrees, so the condition are within the small angle scattering regime.

9. Small angle scattering (SAXS) from a single fibre

In order to understand the SAXS patterns from wood specimens it is helpful first to establish the pattern for a single cellulose fibre placed in an arbitrary orientation relative to the X-ray beam.

In Fig. 13 the plane of the detector is indicated and the incident X-ray beam is shown parallel to the normal to the detector plane. The single fibre f lies in a cell wall indicated by the dotted rectangle. Its normal lies in the x-y plane at an angle α to x and to the direction of the incident X-ray beam which is the vector $\boldsymbol{i}$. The fibre lies at the angle M, the micro-fibril angle, to the z axis which is also the axial direction of the wood cell. Whatever the orientation of the fibre, the small angle scattering will always be in the plane of the cross-section of the cellulose fibre. So the orientation of the scattering streak in the detector plane will be along the line of intersection of the plane of the fibre cross-section and the detector plane. That will be the vector $\boldsymbol{S}$ in Fig. 13 which lies at the azimuth angle ϕ to the equatorial direction y.

Now $\boldsymbol{s}$ is perpendicular to $\boldsymbol{i}$ so the direction cosines of the vector $\boldsymbol{s}$ are

$$(0, \cos\phi, -\sin\phi)$$

for the geometry of Fig. 13.

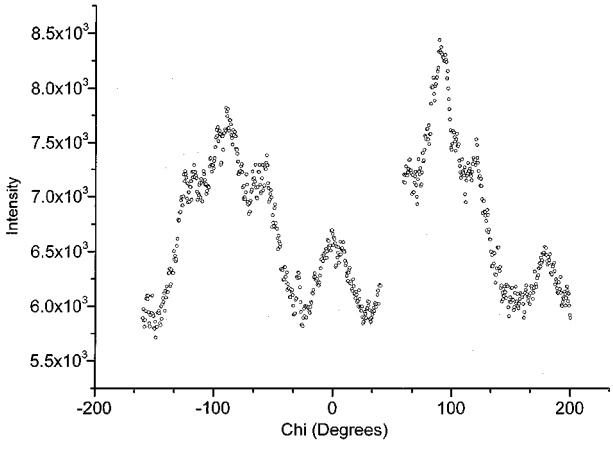

Figure 12 Intensity variation round the (002) diffraction circle for a pinus radiata specimen with the X-ray beam directed normal to one set of cell walls.

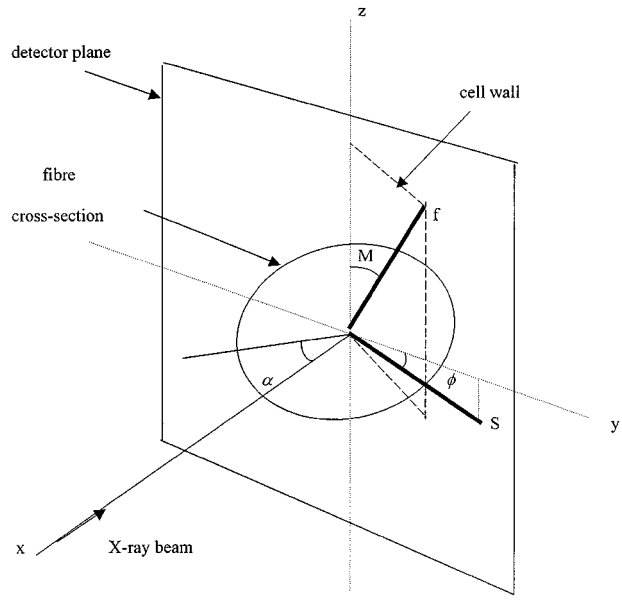

Figure 13 Diagram showing the orientation of the SAXS streak S from a single fibre of arbitrary orientation relative to the X-ray beam.

The direction cosines of $\boldsymbol{f}$, the axis of the fibre, are

$$(\sin M \ \sin\alpha, \sin M \ \cos\alpha, \cos M)$$

The vectors $\boldsymbol{s}$ and $\boldsymbol{f}$ are perpendicular because s lies in the cross-section of $\boldsymbol{f}$, so their scalar product is zero, that is

$$\boldsymbol{s} \cdot \boldsymbol{f} = \cos\phi \ \sin M \ \cos\alpha - \sin\phi \ \cos M = 0$$

or

$$\tan\phi = \cos\alpha \ \tan M \tag{3a}$$

If $\alpha = 0$, that is the X-ray beam is normal to the cell wall, $\phi = M$ and the azimuth angle is equal to the micro-fibril angle.

If $\alpha = 90$ degrees, that is the X-ray beam is parallel to the cell wall, $\phi = 0$ and the scattering streak lies in the equatorial plane.

If $\alpha = 45$ degrees,

$$\tan\phi = \frac{1}{\sqrt{2}} \tan M \tag{3b}$$

10. Scattering from wood samples

Consider now the SAXS pattern that would be produced if the X-ray beam were incident perpendicular to one set of cell walls in a wood specimen with the cell axes vertical. The other set of cell walls would be parallel to the X-ray beam.

The front walls would produce scattering streaks at $\phi = M$ from the two sets of fibres in the S2 layers (see Fig. 14).

The S2 fibres will produce the streaks labelled S2 in Fig. 14. The fibres in the S1 and S3 layers, which

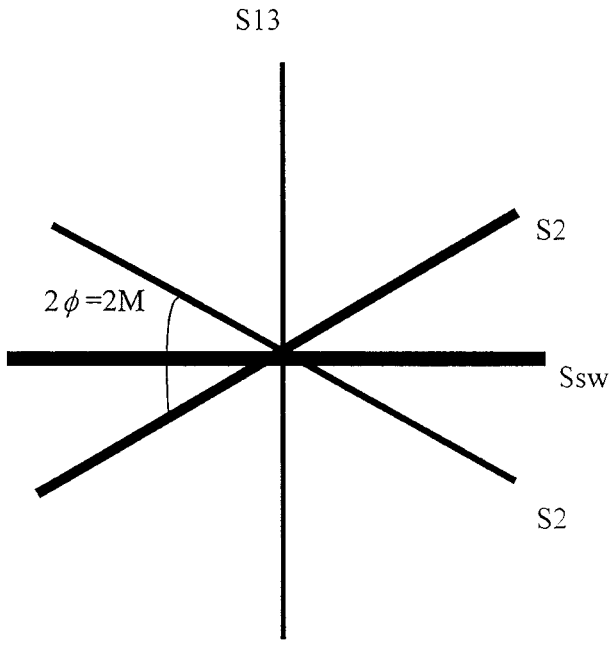

Figure 14 Orientation of all the SAXS streaks from all the cell wall layers in wood cells irradiated with the X-ray beam normal to one set of cell walls.

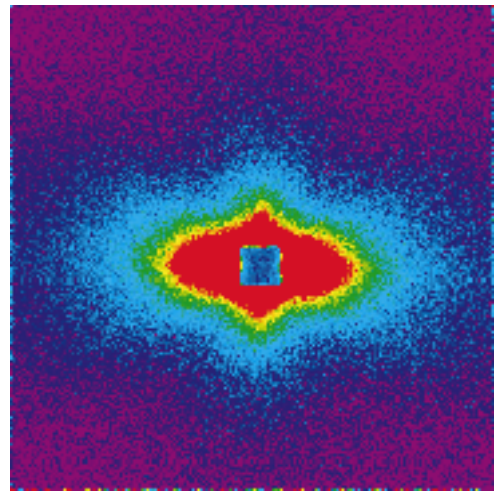

Figure 15 Small angle X-ray scattering pattern for a pinus radiata specimen with the X-ray beam directed normal to one set of cell walls.

are both nearly horizontal will give the vertical streak S13 and the sidewalls will produce a strong horizontal streak Ssw.

To measure the micro-fibril angle we need to measure the angle between the two S2 streaks which is $2\phi = 2M$. Between these two S2 streaks lies the very strong scattering from the side walls Ssw, which conceal part of the S2 streaks. This is illustrated in Fig. 15 which reproduces a SAXS pattern from a pinus radiata specimen with its cell axes vertical and the incident X-ray beam directed normally to one set of cell walls. The SAXS measurements were carried out on the Daresbury Synchrotron with an X-ray wavelength of 0.15 nm and a camera length of 1.75 m. There is a strong lobe of scattering in the equatorial direction from the side walls that obscures the scattering cross from the S2 fibrils. There is also a strong lobe in the direction of the meridian from the S1-S3 layers. It is not possible to extract a value of M from this pattern.

The way round this difficulty is to direct the X-ray beam at an angle of 45 degrees to both sets of cell walls with the cell axes vertical. Then the S2 scattering streaks from the two sets of cell walls superimpose, there is no scattering between the streaks and the angle between the streaks 2ϕ is clearly measurable.

The four sets of S2 fibres are identified in Fig. 9 in the WAXS section, and in Fig. 16 we define the small-angle streaks associated with each set. We have also shown the streak in the meridian plane from the S1 and S3 fibres. This does not obscure the geometry of the S2 cross. The angle between the two S2 streaks, 2ϕ, is indicated in Fig. 16. The azimuth angle ϕ is related to the micro-fibril angle M by Equation 3b:

$$\tan\phi = \frac{1}{\sqrt{2}} \tan M.$$

The SAXS pattern in Fig. 17 was obtained from a pinus radiata specimen 2 mm square cut from the early wood in the 12th growth ring of a tree. The X-ray beam was directed at 45 degrees to both sets of cell walls and the cruciform scattering from the S2 fibres is clearly revealed. There is also evidence of broad streaking from the S1

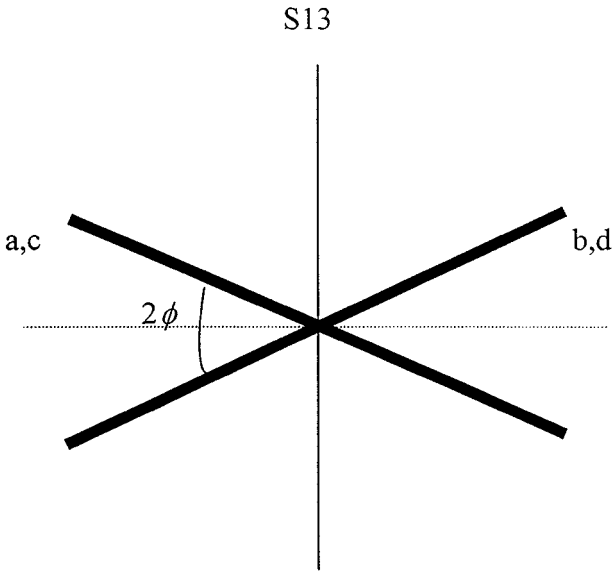

Figure 16 Orientation of the SAXS streaks for the four sets of fibres in the S2 layers with the X-ray beam directed at 45 degrees to both sets of cell walls.

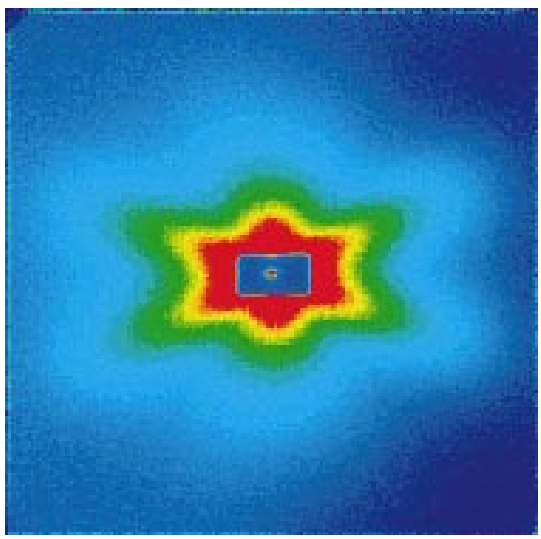

Figure 17 Small angle X-ray scattering pattern from a specimen of pinus radiata 2 mm square from the early wood of the 12th growth ring of the tree. The X-ray beam was directed at 45 degrees to both sets of cell walls.

and S3 fibres in the meridian direction, but this does not obscure the S2 cross. Fig. 18 shows an azimuthal intensity plot through the arms of the S2 cross and the S1-3 streak. Sharp intensity peaks are evident at the centres of the arms of the S2 cross.The precise location of the peak intensity was obtained by fitting Gaussian peaks to the intensity distribution. These are shown in Fig. 18. The two values of 2ϕ measured from the separation of these peaks are 42.4 degrees and 40.1 degrees. The mean value of ϕ is 20.6 degrees. This corresponds to a micro-fibril angle of

$$M = \text{A tan}\left(\frac{\tan 20.6}{\cos 45}\right) = 28.0 \text{ degrees}$$

The SAXS pattern for another pinus radiata specimen is displayed in Fig. 19 and the azimuthal distribution of intensity through the arms of the S2 cross is shown

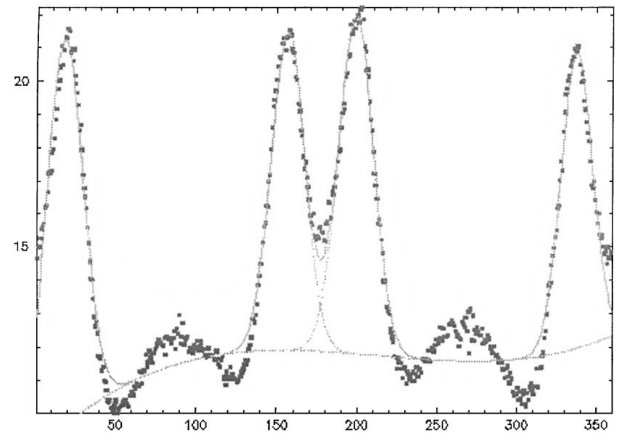

Figure 18 Azimuthal variation of intensity through the arms of the S2 cross and the S1-3 scatter of Fig. 17.

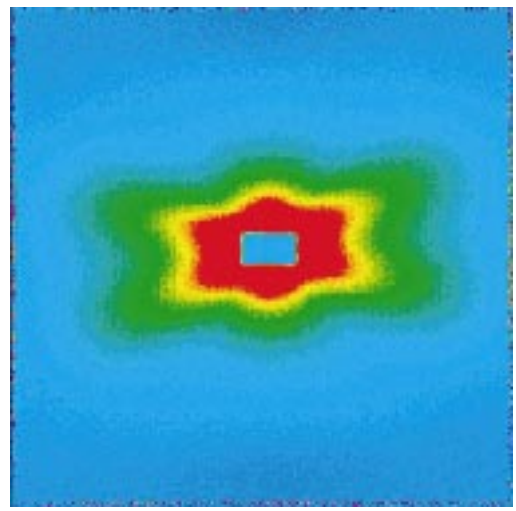

Figure 19 SAXS pattern for another pinus radiata specimen with irradiation conditions similar to those of Fig. 17.

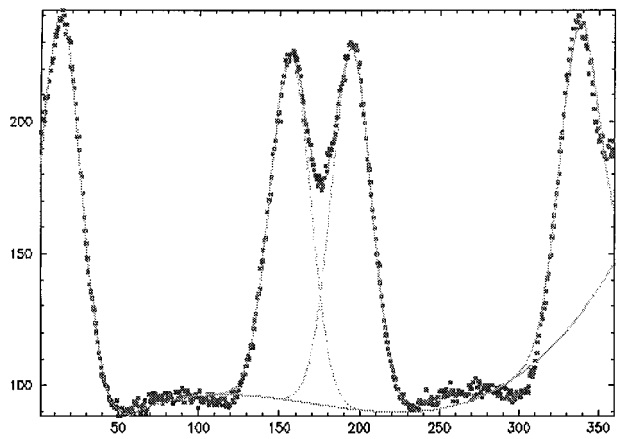

Figure 20 Azimuthal plot of the intensity variation through the S2 scattering cross and the S1-3 scatter of Fig. 19

in Fig. 20. The mean value of the two values of ϕ is 18.2 degrees, corresponding to a value of $M = 24.9$ degrees.

To check the validity of the relation between M, α and ϕ of Equation 3a, a specimen of ramie leaf with parallel cellulose fibres was fixed to the top of a goniometer with a vertical axis of rotation. The fibres were oriented at 40 degrees to the vertical. This simulates a single cell

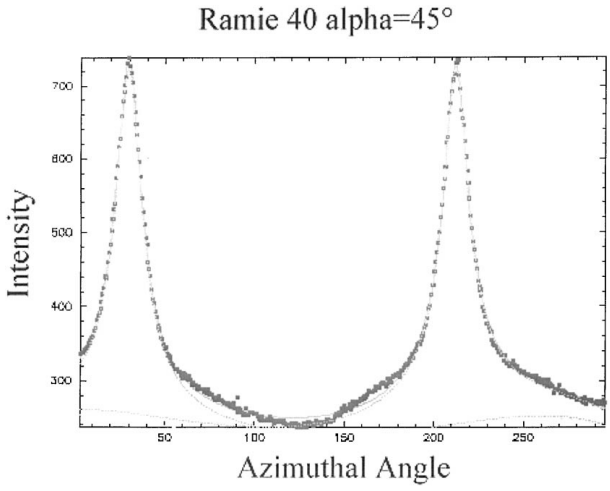

Figure 21 Azimuthal scan through SAXS streaks from fibres with $M = 40^\circ$ and $\alpha = 45^\circ$.

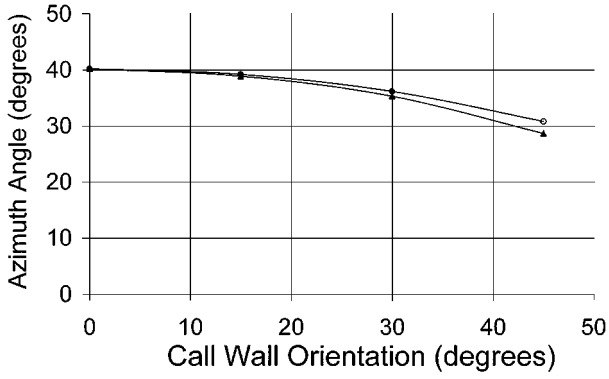

Figure 22 Variation of SAXS azimuth angle with cell wall orientation.

wall with only one set of S2 fibres at a micro-fibril angle of 40 degrees. The plane of the leaf is the plane of the cell wall. The specimen was placed in the X-ray beam and the angle of incidence α of the beam could be varied by rotating the goniometer head. The SAXS pattern comprised a single scattering streak extending beyond a central scattering region. The azimuth angle for the single streak was measured from an azimuthal intensity plot through the streak. Fig. 21 is an example of the case where $\alpha = 45$ degrees. The angles which the two arms of the scattering streaks make with the equatorial direction are 32.0 and 29.7 degrees, giving a mean value of 30.8 degrees. The expected value is

$$\text{A}\tan(\cos 45^* \tan 40) = 30.7 \text{ degrees}.$$

The azimuth angle for a number of values of α is plotted in Fig. 22. The points plotted as circles are the values calculated from Equation 3a and the triangles are the measured values. The agreement between the predicted and the measured values is seen to be satisfactory.

11. Conclusion

It has been demonstrated that small angle scattering patterns obtained with the X-ray beam equally inclined to the two sets of cell walls constitutes a direct, simple and unambiguous method for the measurement of micro-fibril angles in softwood. Using a powerful facility such as the the Daresbury Synchtron, the radiation generated by the acceleration of the 2 Gev electrons permits data of excellent quality to be gathered in at most five minutes.

The method we have proposed using wide angle diffraction from a specimen with the cell walls oriented at 45 degrees to the X-ray beam has been shown to be capable of yielding micro-fibril angle values. Its advantage over the method that irradiates the specimen normal to one set of call walls is that it is not necessary to estimate the background intensity.

The methods we have explored in the work now described assume that there are two orthogonal sets of cell walls in softwood. Micrographs of cell structures reveal that this is not always precisely the case. We plan to explore, by measuring cell wall orientation distributions in specimens of pinus radiata, to what degree the diffraction patterns from characterised real structures will differ from those from the simple structures we have assumed.

Acknowledgements

The authors acknowledge with gratitude the support received during the progress of this work from the staff of the CLRC Synchrotron Laboratory at Daresbury, particularly from Dr Liz Towns-Andrew and Mr. Anthony Gleeson. They are grateful for the assistance they received in the X-ray facility of the Manchester Materials Science Centre from Mr. Ian Brough and for access to Professor Ward Robinson's X-ray facility in the Chemistry Department of the University of Canterbury in New Zealand. Ms. Jan Wakaira was particularly helpful.

References

1. B. A. MEYLAN, *Forest Products Journal* **17** (1967) 51.
2. C. YE and O. SUNDSTROM, *Tappi Journal* **80** (1997) 181.
3. W. PLAESANTS, W. J. BATCHELOR and I. H. PARKER, *Appita Journal* **51** (1998) 3733.
4. I. D. CAVE, *Forest Products Journal* **16** (1966) 37.

Received 5 January
and accepted 11 August 1999